Dielectric relaxation in epitaxial films of paraelectric-magnetic $SrTiO_3$-$SrMnO_3$ solid solution

M. Savinov, V. Bovtun, E. Tereshina-Chitrova, A. Stupakov, A. Dejneka, and M. Tyunina

Citation: Appl. Phys. Lett. **112**, 052901 (2018);
View online: https://doi.org/10.1063/1.5017667
View Table of Contents: http://aip.scitation.org/toc/apl/112/5
Published by the American Institute of Physics

Dielectric relaxation in epitaxial films of paraelectric-magnetic $SrTiO_3$-$SrMnO_3$ solid solution

M. Savinov,[1] V. Bovtun,[1] E. Tereshina-Chitrova,[1] A. Stupakov,[1] A. Dejneka,[1] and M. Tyunina[2,1,a)]
[1]*Institute of Physics of the Czech Academy of Sciences, Na Slovance 2, 18221 Prague, Czech Republic*
[2]*Microelectronics Research Unit, Faculty of Information Technology and Electrical Engineering, University of Oulu, P. O. Box 4500, FI-90014 Oulu, Finland*

(Received 29 November 2017; accepted 16 January 2018; published online 29 January 2018)

Magneto-dielectric properties of $(A^{2+})MnO_3$-type perovskites are attractive for applications and stimulate extensive studies of these materials. Here, the complex dielectric and magnetic responses are investigated as in epitaxial films of $SrTi_{0.6}Mn_{0.4}O_3$, solid solution of paraelectric $SrTiO_3$ and magnetic $SrMnO_3$. The impedance and resonance measurements at frequencies of 10^{-2}–10^{10} Hz and temperatures of 10–500 K reveal broad dielectric anomalies centered at 100–200 K, while the films are paramagnetic at all temperatures. Analysis shows polaronic electrical conductivity behind the observed behavior. Electron-phonon correlations, rather than spin-phonon correlations, are suggested to produce the apparent magneto-dielectric responses in many multiferroic manganites. *Published by AIP Publishing.* https://doi.org/10.1063/1.5017667

Coexistence and coupling of dipolar and spin orderings in a single-phase material are attractive for applications, intriguing fundamentally, and stimulate tremendous scientific interest in magnetoelectric multiferroics.[1–5] In particular, single-phase $AMnO_3$-type perovskite multiferroics (A = Ba, Sr, etc.), including (Sr,Ba)MnO_3, Sr(Mn,Ti)O_3, and others, are intensively studied.[6–30] Magnetic-dielectric coupling is manifested by similar temperatures of the dielectric anomalies and magnetic ordering and ascribed to strong spin-phonon correlations in these materials.[6–12,20,25,26] Concurrently, a magnetic-field-dependent electrical conduction of undescribed origin was also shown to produce typical magneto-dielectric response.[27] We note that (Sr,Ba)MnO_3, (Sr,Ca)MnO_3, and Sr(Mn,Ti)O_3 systems exhibit profound conductivity, the mechanism of which is under debate.[7,8,21,23,25,30] In this letter, we show that electron-phonon correlations cause polaronic electrical conduction, which may mimic magneto-dielectric behavior in many multiferroic manganites. We investigate dielectric relaxation at frequencies of 10^{-2}–10^{10} Hz and temperatures of 10–500 K in epitaxial films of $SrTi_{0.6}Mn_{0.4}O_3$ (STMO), solid solution of paraelectric $SrTiO_3$ (STO) and magnetic $SrMnO_3$. For this Ti:Mn ratio, STMO possesses a cubic perovskite structure.[28,29] We observe broad dielectric anomalies centered at 100–200 K, while the films are paramagnetic insulators at all temperatures. We demonstrate that universal relaxation of electrical conductivity produces these anomalies. We also show the polaronic mechanism of conductivity, which implies the presence of strong electron-phonon correlations in the films. We suggest that the magneto-dielectric behavior may result from the electron-phonon correlations instead of (or in addition to) the spin-phonon correlations in many multiferroic manganites.

STMO films were prepared by pulsed laser deposition on top of (001)-oriented single crystals of $(La_{0.18}Sr_{0.82})(Al_{0.59}Ta_{0.41})O_3$ (LSAT) and pure insulating and Nb-doped (0.7 wt. %) conducting $SrTiO_3$ (STO) (MTI Corp.). A ceramic mixture of $SrTiO_3$ and $SrMnO_3$ was used as the target. The theoretical STMO-substrate lattice misfit is zero for LSAT and tensile <1% for STO substrates. Correspondingly, cube-on-cube-type epitaxial perovskite films of STMO were grown pseudomorphically to the thicknesses of 200 nm and 100 nm on LSAT and STO, respectively. The crystal structure is cubic (lattice parameter ~0.386 nm) in the STMO/LSAT film and metrically tetragonal (out-of-plane lattice parameter ~0.384 nm) in the STMO/STO film. Chemical Ti:Mn ordering or formation of a double-perovskite phase is not detected in the films. Details on microstructural characterization of the films are shown in the supplementary material.

Magnetic and electric properties of the films were inspected in the broad range of conditions. Magnetic measurements were performed on a Quantum Design SQUID magnetometer (MPMS XL 7T) at the temperatures of 1.8–300 K and magnetic fields to 3 T. Reciprocating sample transport with the magnetic sensitivity of 10^{-8} emu was used. To examine the electric properties of the STMO/LSAT film without electrodes, a thin dielectric resonator method was applied.[31] A reference bare LSAT substrate and the resonance frequency of 12.7 GHz were used. The measurements were performed using an Agilent E8364B vector network analyzer in a JANIS closed-cycle He cryostat. The film's response was obtained as a product ($\varepsilon\mu$) of the complex dielectric permittivity and magnetic permeability. The conducting STO substrate and pulsed-laser-deposited Pt pads acted as the bottom and top electrodes, respectively, for the STMO/STO film. The impedance of the Pt/STMO/STO capacitors was measured using a NOVOCONTROL Alpha-AN high performance frequency analyzer. The real part of the dielectric permittivity (ε'), loss factor (tan D), and real part of ac conductivity (σ) was obtained considering a leaky parallel-plate capacitor. The temperature control was

a)Author to whom correspondence should be addressed: marina.tjunina@oulu.fi and tjunina@fzu.cz

realized using a JANIS ST-100 He flow cryostat equipped with a LakeShore 335 temperature controller. The results of electrical characterization were analyzed using various theoretical models of conduction.[32–37]

After subtracting the linear diamagnetic signals from the total measured ones, paramagnetic-type behavior is found in the STMO films [Figs. 1(a) and 1(d)]. The temperature dependence of the small-signal magnetization, determined on cooling at 0.01 T, is smooth, free of any anomalies, and possesses a typical hyperbolic shape. The magnetization-field loops are also of paramagnetic character and consistent with those in disordered $SrTi_{0.5}Mn_{0.5}O_3$ ceramics.[21] Additional cooling in the magnetic field of 3 T has not revealed any new features.

The real and imaginary parts of the complex response ($\varepsilon\mu$) of the STMO/LSAT film evidence a broad anomaly around 200 K [Figs. 1(b) and 1(c)]. The anomaly contrasts to the smooth paramagnetic curve in Fig. 1(a) and, hence, can be ascribed to the electrical, rather than magnetic, properties of STMO.

In the STMO/STO film, the broad anomalies around 200 K are observed in the temperature dependence of the permittivity [Fig. 1(e)], loss, and conductivity [Fig. 1(f)]. Again, these anomalies are in contrast to the smooth magnetization curve [Fig. 1(d)].

In addition to the broad anomalies at ~200 K, a profound increase in the permittivity with increasing temperature above 300 K is seen in the STMO/LSAT and STMO/STO films. Such behavior is often observed at high temperatures in perovskite oxide ferroelectrics, where carriers, trapped on deep-level defect states, are thermally released.[37] The conductivity rises correspondingly [Fig. 1(f)].

The broad electric anomalies possess strong frequency dispersion [Fig. 2]. We stress that this dispersion is clearly separated from the high-temperature conductivity-related dispersion [compare Figs. 2(b) and 2(c)]. The temperatures T_m of maxima in the permittivity [Fig. 2(a)], loss [Fig. 2(b)], and conductivity shift to higher temperatures with increasing measurement frequency f. An Arrhenius-type relationship $f = f_0 \exp(-E_A/k_B T_m)$ is found by plotting $\ln(f)$ as a function of inverse temperatures $(T_m)^{-1}$ [Figs. 2(d) and 2(e)]. Here, f_0, E_A, and k_B are the attempt frequency, activation energy, and Boltzmann constant, respectively. The fitted values are approximately $f_0 \approx 10^{11}$ Hz and $E_A \approx$ (0.1–0.2) eV.

To get better insight in the nature of the electric anomalies, the conductivity σ is analyzed in more detail. First, log-log plots of ac conductivity versus frequency reveal a power-law behavior [Fig. 3(a) and supplementary material]. Good fits to universal relaxation in the form $[\sigma = \sigma_0 + A\omega^{s}]$ are obtained at all temperatures.[32] Here, σ_0 is the dc conductivity, s is the exponent, and ω is the angular frequency $\omega = 2\pi f$. Note that the low-frequency ac conductivity and the fitted dc conductivity are small, $\sim 10^{-9}$ S cm^{-1}, at room temperature and decrease on cooling. The magnitude of the conductivity evidences that the STMO films are insulators. The power-law relaxation [Fig. 3(a)] is typical for numerous disordered insulators.

Here, the exponent s is temperature-independent and close to unity at temperatures $T > 150$ K [Fig. 3(b)]. This behavior

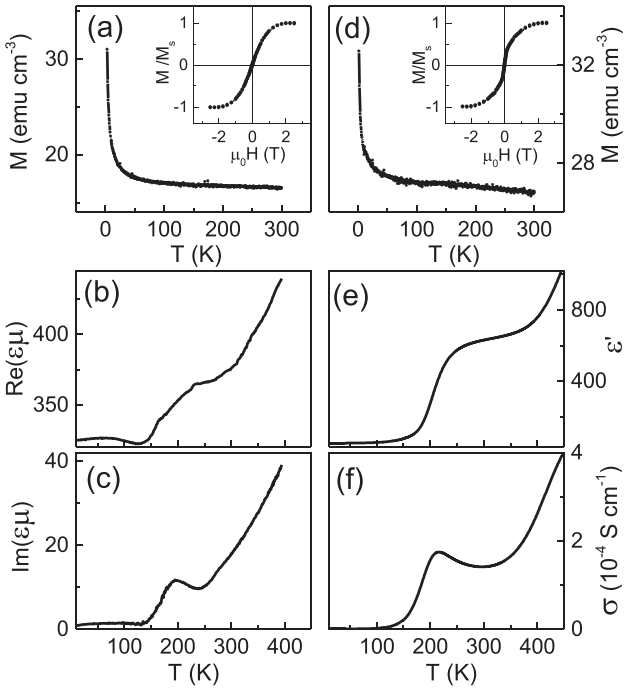

FIG. 1. (a) and (d) Magnetic and (b), (c), (e), and (f) electric properties as a function of temperature in the (a)–(c) STMO/LSAT and (d)–(f) STMO/STO films. (a) and (d) Magnetization M as a function of temperature T at 0.01 T and (insets) normalized magnetization as a function of magnetic field at 10 K. (b) Real and (c) imaginary parts of the complex microwave response at a frequency of 12.7 GHz. (e), (f) Real parts of the (e) dielectric permittivity and (f) ac conductivity at a frequency of 1 MHz.

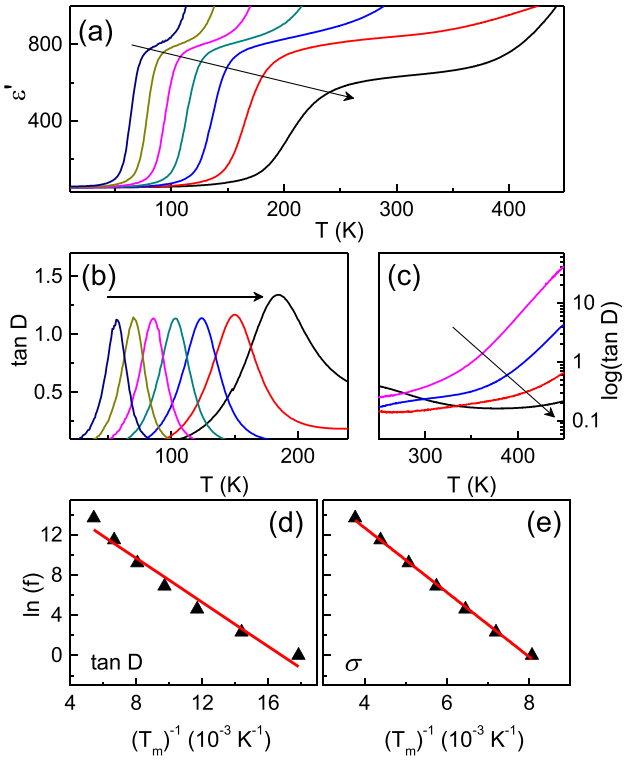

FIG. 2. Frequency dispersion of the dielectric response in the STMO/STO film. (a) Real part of the dielectric permittivity ε' and (b) and (c) loss factor tan D as a function of temperature at frequencies (a) and (b) 1 Hz–1 MHz and (c) 1 Hz–1 kHz. The arrows show the directions of frequency increase. (d) and (e) Relationship between frequencies and temperatures T_m of maxima in (d) tan D and (e) ac conductivity. Lines show fits to the Arrhenius law.

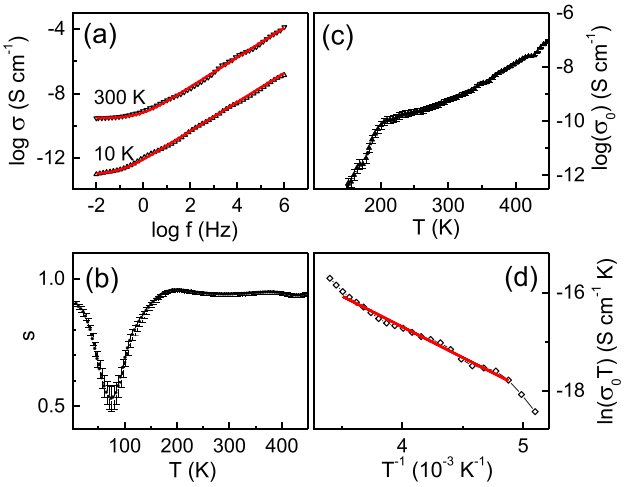

FIG. 3. Conductivity in the STMO/STO film. (a) Log-log plots of ac conductivity versus frequency at different temperatures. Solid curves show fits to universal relaxation law. (b) Exponent s and (c) dc conductivity σ_0 as a function of temperature. (d) Relationship between $\ln(\sigma_0 T)$ and inverse temperature. The solid line shows fit to polaronic hopping.

of s indicates that phonon-assisted quantum-mechanical tunneling, or polaron tunneling, is the mechanism of ac conductivity (see, e.g., Ref. 33 and references therein). A minimum exhibited by the exponent s at temperatures around 75 K implies tunneling (hopping) of large, or overlapping, polarons.

Next, the presence of polarons is corroborated by the behavior of dc conductivity σ_0 [Figs. 3(c) and 3(d)]. The conductivity σ_0 was analyzed at temperatures between 200 and 300 K, where the influence of the high-temperature conductivity and overlapping polarons is minor. Different models including adiabatic polaronic hopping $[\sigma_0 T \propto \exp(-E_H/k_B T)]$, Mott-type variable range hopping $[\sigma_0 T^{1/4} \propto \exp\{-(T_M/T)^{1/4}\}]$, and Efros–Shklovskii hopping $[\sigma_0 T^{1/2} \propto \exp\{-(T_{ES}/T)^{1/2}\}]$ were applied.[34–36] Although fits to the Mott and Efros–Shklovskii models are satisfactory, the obtained characteristic temperatures T_M and T_{ES} and hopping energies appear extremely large, discarding these mechanisms (supplementary material). The polaronic hopping is confirmed by the good fit [Fig. 3(d)] and reasonable activation energy $E_H \approx 0.1$ eV.

Our observations imply that polaronic hopping is responsible for the frequency and temperature dependent conductivity, leading to the apparent dielectric anomalies in the STMO films. Because polarons are known to result from electron-lattice (or electron-phonon) correlations, the dielectric anomalies evidence the presence of electron-phonon, rather than spin-phonon, correlations here. Note that the shape of the dielectric anomalies in our films [Figs. 1(b), 1(c), and 1(e)] is remarkably similar to that in thin epitaxial $Sr_{0.6}Ba_{0.4}MnO_3$ films.[20] The anomalies were considered as a proof for spin-phonon coupling in those films.[20] However, the lack of conductivity data makes this interpretation incomplete, because electron-phonon coupling may give the same apparent electrical behavior.

It is worth mentioning that strong electron-phonon correlations produce stable polarons in manganites of $(Re_{1-x}A_x)MnO_3$-type, where Re and A stand for the rare-earth and alkaline cations, respectively.[34,38–40] The polaronic conductivity is sensitive to the applied magnetic field and contributes significantly to magneto-resistance in these manganites. The presence of magnetic polarons is manifested in magneto-optical behavior as well.[41,42] Such polarons are related to electrons trapped in narrow d-orbitals of Mn, indicating that many manganites may exhibit magneto-polaronic effects. We therefore argue that magneto-polarons may mimic spin-phonon coupling in multiferroic manganites.

In summary, broad anomalies in the temperature dependence of complex dielectric response are observed at 100–200 K in epitaxial films of $SrTi_{0.6}Mn_{0.4}O_3$, which are paramagnetic insulators at all temperatures. The anomalies are shown to result from polaronic electrical conductivity, implying strong electron-phonon correlations in the films. The electron-phonon correlations, rather than spin-phonon correlations, are suggested to be responsible for magneto-dielectric behavior in many multiferroic manganites.

See supplementary material for details of microstructural characterization and conductivity analyses.

The authors acknowledge support from the Grant Agency of the Czech Republic (Grant No. 15-15123S). Research facilities of the Center for Advanced Functional Materials (SAFMAT) and the Magnetism and Low Temperature Laboratories (MLTL) were employed in this work.

[1]M. Fiebig, J. Phys. D: Appl. Phys. **38**, R123 (2005).
[2]S. Dong, J.-M. Liu, S.-W. Cheong, and R. Zhifeng, Adv. Phys. **64**, 519 (2015).
[3]M. Fiebig, T. Lottermoser, D. Meier, and M. Trassin, Nat. Rev. Mater. **1**, 16046 (2016).
[4]N. A. Spaldin, MRS Bull. **42**, 385 (2017).
[5]J. Fontcuberta, C. R. Phys. **16**, 204 (2015).
[6]O. Chmaissem, B. Dabrowski, S. Kolesnik, J. Mais, D. E. Brown, R. Kruk, P. Prior, B. Pyles, and J. D. Jorgensen, Phys. Rev. B **64**, 134412 (2001).
[7]H. Sakai, J. Fujioka, T. Fukuda, D. Okuyama, D. Hashizume, F. Kagawa, H. Nakao, Y. Murakami, T. Arima, A. Q. R. Baron, Y. Taguchi, and Y. Tokura, Phys. Rev. Lett. **107**, 137601 (2011).
[8]D. K. Pratt, J. W. Lynn, J. Mais, O. Chmaissem, D. E. Brown, S. Kolesnik, and B. Dabrowski, Phys. Rev. B **90**, 140401(R) (2014).
[9]J. H. Lee and K. M. Rabe, Phys. Rev. Lett. **104**, 207204 (2010).
[10]J. Hong, A. Stroppa, J. Íñiguez, S. Picozzi, and D. Vanderbilt, Phys. Rev. B **85**, 054417 (2012).
[11]T. Günter, E. Bousquet, A. David, Ph. Boullay, Ph. Ghosez, W. Prellier, and M. Fiebig, Phys. Rev. B **85**, 214120 (2012).
[12]C. Becher, L. Maurel, U. Aschauer, M. Lilienblum, C. Magen, D. Meier, E. Langenberg, M. Trassin, J. Blasco, I. P. Krug, P. A. Algarabel, N. A. Spaldin, J. A. Pardo, and M. Fiebig, Nat. Nanotechnol. **10**, 661 (2015).
[13]L. Maurel, N. Marcano, T. Prokscha, E. Langenberg, J. Blasco, R. Guzmán, A. Suter, C. Magén, L. Morellón, M. R. Ibarra, J. A. Pardo, and P. A. Algarabel, Phys. Rev. B **92**, 024419 (2015).
[14]R. U. Chandrasena, W. Yang, Q. Lei, M. U. Delgado-Jaime, K. D. Wijesekara, M. Golalikhani, B. A. Davidson, E. Arenholz, K. Kobayashi, M. Kobata, F. M. F. de Groot, U. Aschauer, N. A. Spaldin, X. Xi, and A. X. Gray, Nano Lett. **17**, 794 (2017).
[15]E. Bousquet and A. Cano, J. Phys.: Condens. Matter **28**, 123001 (2016).
[16]J. Schaab, I. P. Krug, H. Doğanay, J. Hackl, D. M. Gottlob, M. I. Khan, S. Nemšák, L. Maurel, E. Langenberg, P. A. Algarabel, J. A. Pardo, C. M. Schneider, and D. Meier, Phys. Rev. Appl. **5**, 054009 (2016).
[17]R. Guzmán, L. Maurel, E. Langenberg, A. R. Lupini, P. A. Algarabel, J. A. Pardo, and C. Magén, Nano Lett. **16**, 2221 (2016).
[18]P. Agrawal, J. Guo, P. Yu, C. Hébert, D. Passerone, R. Erni, and M. D. Rossell, Phys. Rev. B **94**, 104101 (2016).
[19]E. Langenberg, R. Guzman, L. Maurel, L. Martinez de Banos, L. Morellon, M. R. Ibarra, J. Herrero-Martin, J. Blasco, C. Magen, P. A. Algarabel, and J. A. Pardo, ACS Appl. Mater. Interfaces **7**, 23967 (2015).

[20]V. Goian, E. Langenberg, N. Marcano, V. Bovtun, L. Maurel, M. Kempa, T. Prokscha, J. Kroupa, P. A. Algarabel, J. A. Pardo, and S. Kamba, Phys. Rev. B **95**, 075126 (2017).
[21]I. Qasim, P. E. R. Blanchard, B. J. Kennedy, C. D. Ling, L.-Y. Jang, T. Kamiyama, P. Miao, and S. Torii, Dalton Trans. **43**, 6909 (2014).
[22]I. Alvarez-Serrano, M. A. Arillo, M. Garcia-Hernandez, M. L. Lopez, C. Pico, and M. L. Veiga, J. Am. Ceram. Soc. **93**, 2311 (2010).
[23]I. Alvarez-Serrano, M. L. Lopez, F. Rubio, M. Garcia-Hernandez, G. J. Cuello, C. Pico, and M. L. Veiga, J. Mater. Chem. **22**, 11826 (2012).
[24]J. Lamsal, R. Mondal, A. Kumar, K. K. Bharathi, P. N. Santhosh, R. Nirmala, A. K. Nigam, W. B. Yelon, S. Quezado, and S. K. Malik, J. Appl. Phys. **109**, 07E329 (2011).
[25]K. R. S. P. Meher, M. Savinov, S. Kamba, V. Goian, and K. B. R. Varma, J. Appl. Phys. **108**, 094108 (2010).
[26]S. Kamba, V. Goian, V. Skoromets, J. Hejtmanek, V. Bovtun, M. Kempa, F. Borodavka, P. Vanek, A. A. Belik, J. H. Lee, O. Pacherova, and K. M. Rabe, Phys. Rev. B **89**, 064308 (2014).
[27]E. Langenberg, I. Fina, J. Ventura, B. Noheda, M. Varela, and J. Fontcuberta, Phys. Rev. B **86**, 085108 (2012).
[28]A. Karaphun, S. Hunpratub, T. Putjuso, and E. Swatsitang, Jpn. J. Appl. Phys., Part 1 **54**, 06FH09 (2015).
[29]V. Trepakov, M. Makarova, O. Stupakov, E. A. Tereshina, J. Drahokoupil, M. Cernansky, Z. Potucek, F. Borodavka, V. Valvoda, A. Lynnyk, A. Jager, L. Jastrabik, and A. Dejneka, Mater. Chem. Phys. **143**, 570–577 (2014).
[30]K. R. S. P. Meher and K. B. R. Varma, J. Appl. Phys. **105**, 034113 (2009).
[31]V. Bovtun, V. Pashkov, M. Kempa, S. Kamba, A. Eremenko, V. Molchanov, Y. Poplavko, Y. Yakymenko, J. H. Lee, and D. G. Schlom, J. Appl. Phys. **109**, 024106 (2011).
[32]A. K. Jonscher, *Universal Relaxation Law* (Chelsea Dielectrics Press, 1995).
[33]A. Ghosh, Phys. Rev. B **41**, 1479 (1990).
[34]D. M. Edwards, Adv. Phys. **51**, 1259 (2002).
[35]N. F. Mott and E. A. Davis, *Electronic Processes in Non-Crystalline Materials* (Clarendon Press, Oxford, 1971).
[36]A. L. Efros and B. I. Shklovskii, J. Phys. C: Solid State Phys. **8**, L49 (1975).
[37]C. Ang, Z. Yu, and L. E. Cross, Phys. Rev. B **62**, 228 (2000).
[38]J. M. D. Coey, M. Viret, and S. von Molnar, Adv. Phys. **48**, 167 (1999).
[39]M. B. Salomon and M. Jaime, Rev. Mod. Phys. **73**, 583 (2001).
[40]E. Dagotto, Phys. Rep. **344**, 1 (2001).
[41]J. M. Caicedo, J. Fontcuberta, and G. Herranz, Phys. Rev. B **89**, 045121 (2014).
[42]B. Casals, R. Cichelero, P. G. Fernandez, J. Junquera, D. Pesquera, M. Campoy-Quiles, I. C. Infante, F. Sanchez, J. Fontcuberta, and G. Herranz, Phys. Rev. Lett. **117**, 026401 (2016).